

INVESTIGATION INTO VIBRATION BEHAVIOR OF THE INTEGRATED SHALLOT HARVESTER

KHẢO SÁT ĐỘNG LỰC HỌC DAO ĐỘNG CỦA LIÊN HIỆP MÁY THU HOẠCH HÀNH TÍM

Dang NguyenTH¹⁾, Phi CaoH²⁾, Hung TranV³⁾, Hau LeT⁴⁾, Giang Pham TT⁵⁾

^{1,2,4)} Faculty of Mechanical Engineering, Vinh Long University of Technology Education/ Vietnam

⁵⁾ Faculty of Basic Science, Vinh Long University of Technology Education/ Vietnam

³⁾ Faculty of Mechanical Engineering, Phenikaa University/ Vietnam

Corresponding author: Dang NguyenTH

Tel: 0917499199; E-mail: dangnth@vlute.edu.vn

DOI: <https://doi.org/10.35633/inmateh-76-50>

Keywords: Integrated shallot harvester, 17-dof model, vibration dynamics, harvesting depth, Bekker soil sinkage

ABSTRACT

The study investigates the vibration dynamics of the integrated shallot harvesting machine to support design refinement, aiming to improve operational efficiency, harvesting performance, and packaging for transportation. The investigation is based on an existing integrated machine developed under a Vietnamese State-Level Scientific Research Project. A dynamic model with 17 degrees of freedom was developed to comprehensively represent the system's motion, including the tractor, harvester, harvesting head, coupling joint, and eight wheels. Nonlinear soil characteristics were modeled using the Bekker terrain model, with specific soil parameters measured in Vietnam fields. Simulation results show notable vibrations in the integrated shallot harvesting machine and the harvesting head. At the beginning of the harvesting phase, the head experiences large amplitudes and high accelerations, which may damage shallot bulbs. The study proposes technical solutions such as optimizing damping coefficients, adjusting system stiffness, or incorporating active control systems to maintain stable harvesting depth and improve harvesting quality. The results provide a foundation for further refinement of integrated shallot harvesting machine design.

TÓM TẮT

Nghiên cứu động lực học liên hiệp máy thu hoạch hành tím thông qua khảo sát các thông số dao động sẽ góp phần hoàn thiện thêm thiết kế nhằm tăng thêm hiệu quả hoạt động và tăng năng suất thu hoạch cũng như đóng gói và vận chuyển. Phương pháp khảo sát dựa trên liên hiệp máy hiện có là sản phẩm của đề tài nghiên cứu khoa học cấp Nhà nước Việt Nam. Một mô hình động lực học được phát triển với 17 bậc tự do mô tả đầy đủ chuyển động của hệ thống gồm máy kéo, máy thu hoạch, mũi thu hoạch, khớp nối và 8 bánh xe. Các tính chất phi tuyến của đất ruộng theo mô hình Bekker đã được áp dụng với các hệ số đặc trưng trên đồng ruộng Việt Nam. Kết quả mô phỏng cho thấy dao động của liên hiệp máy và mũi thu hoạch. Ban đầu mũi thu hoạch có biên độ lớn và gia tốc cao sẽ gây hư hỏng củ hành. Nghiên cứu này đề xuất các giải pháp kỹ thuật bao gồm tối ưu hóa hệ số giảm chấn, điều chỉnh độ cứng của hệ thống hoặc bổ sung bộ điều khiển chủ động để duy trì ổn định độ sâu thu hoạch nhằm nâng cao chất lượng thu hoạch hành tím. Các kết quả thu được có thể dùng tham khảo cho hoàn thiện thiết kế liên hiệp máy thu hoạch hành tím.

INTRODUCTION

Shallots (*Allium cepa* var. *aggregatum*) are a high-value crop from the Allium family, cultivated extensively in many countries worldwide. In Vietnam, shallots are considered a specialty seasoning crop with significant economic importance.

In the context of agricultural mechanization, using an integrated shallot harvesting machine (ISHM) during harvesting and transportation phases can enhance labor productivity, reduce manual effort, lower production costs, and contribute to the modernization of agriculture. Developing a dynamic model for this system aims to define its real-world operational characteristics based on an existing ISHM design, thereby assessing the current design and providing essential data for further optimization.

International studies on shallot harvesters have shown that while these machines share general design principles, their specific configurations differ to suit local field conditions and soil properties in each country.

In the study by *Massah & Arabhosseini (2012)*, a design calculation and experimental validation were conducted using the cutting blade angle as the input parameter. The results indicated that setting the blade at an inclination angle of 20° yielded the best performance, as evidenced by the lowest damage rate to shallot bulbs among the tested configurations. An optimized design of the working mechanism in the integrated harvesting machine, combining digging, gathering, and sieving into a single operational unit with sequential automation and no manual intervention, helps reduce overall machine dimensions. It also enhances component modularity, allowing for easy assembly/disassembly, on-field maintenance, and compatibility with small tractors or walk-behind machines. The tip angle of the digging blade and the operating speed of the ISHM directly affect the quality of the harvested shallots. The use of a vibrating V-shaped digging blade with an adjustable angle of 18–21°, controlled via a hand screw mechanism, allows for easy operation and adaptability to various soil types.

In the harvesting study by *Kumawat & Raheman (2023)*, an analysis was conducted based on a dataset of shallot bulb dimensions. It was reported that bulbs with diameters ranging from 44 to 58 mm and weights between 47 and 66 g required an extraction force of 20–25 N. Regarding field conditions, the study found that a soil moisture content of 12% was optimal for harvesting. However, achieving such conditions is often challenging in practice due to unstable weather patterns, particularly the frequent alternation of sun and rain during the period when shallots have fully matured and are ready for harvest.

After being uprooted from the soil, shallot bulbs are transported via conveyors integrated within the machine body to the discharge point above the storage bin. Synchronizing the speed of the uprooting mechanism with the storage bin filling process helps reduce clogging and enhances harvesting efficiency. The synchronization is influenced by the travel speed of the chain and belt conveyors within the harvester. A study by *Erokhin et al. (2022)* addressed the issue and proposed an optimal conveyor speed of 1.7 m/s, which achieved a soil separation efficiency of 98.4%.

In the design process, the structure and shape of the digging blade are also carefully considered, as the forces acting on the blade tip resemble those experienced by a plowshare during soil penetration. The study by *Mehta & Yadav (2015)* demonstrated that a V-shaped digging blade with appropriately designed tip angles provides the lowest draft force, measured at approximately 625.6 N. The study by *Khura & Mani (2011)* reported that an optimal operating speed of approximately 2–4 km/h effectively reduces vibration and prevents mechanical damage to shallot bulbs during harvesting.

In practice, vibration is a major concern during the operation of integrated shallot harvesting machines (ISHM) due to its direct impact on bulb damage, operator health, and machine durability. Vibrations originate from components such as the digging blade, chassis, and rotating or oscillating parts, and are often transmitted through the seat and frame to the operator. The intensity of vibration varies depending on machine design, soil characteristics, and terrain conditions. If not properly controlled, vibration can lead to fatigue and long-term musculoskeletal disorders (*Vlăduț et al., 2023; Vlăduț et al., 2013*). A recent study by *Marin et al. (2024)* applied methods such as acceleration spectrum analysis, RMS calculation, and fatigue prediction models to assess risks and define safe exposure durations in accordance with ISO 2631-1 and 2631-5 standards. Experimental research conducted by *Cârdei et al. (2023)* on soil tillage machines such as the MCLS revealed that vibrations at the working components are random and nonlinear, requiring analysis through statistical tools like spectral density and autocorrelation to identify critical stress zones and propose improvements to the damping system.

Although *Bekker (1969)* foundational work remains the seminal reference on soil behavior and is considered the cornerstone of terramechanics, further studies have pointed out limitations in its practical applications. In particular, *Rashidi et al. (2012)* raised concerns regarding the limitations of the Bekker model in accurately predicting pressure–sinkage responses of soil under real-world conditions, especially when applied directly to wheel–soil interaction in agricultural field studies.

Their research referenced the classic Bekker equation:

$$p = \left(\frac{k_c}{b} + k_\phi \right) z^n \quad (1)$$

where: p : the contact pressure; z : the sinkage; k_c and k_ϕ : soil stiffness coefficients; b : the contact width; n : the sinkage exponent.

To improve the accuracy of dynamic analysis, *Múčka (2018)* combined Bekker's soil sinkage model with ISO 8608 road surface classifications, selecting the appropriate surface type to realistically simulate agricultural field terrain.

MATERIALS AND METHODS

The Integrated Shallot Harvesting Machine

The demand for shallot production in the Mekong Delta region of Vietnam has been supported through a scientific research project under code KHCN-TNB.ĐT/14-19/C29. The authors conducted the design and fabrication of a prototype, followed by field testing. The machine is powered by a KUBOTA L4508VN tractor, operating under stable working conditions. Initial evaluations have demonstrated the design's suitability for shallot fields in the Mekong Delta. An image of the machine is shown in Fig. 1 (Phi et al. 2021).



Fig. 1 - Research Prototype of the Designed and Fabricated Machine

The specifications of the ISHM, as cited by the project leader and the research team, are presented in Table 1 (Phi et al., 2022; Phi et al., 2020).

Table 1

Basic Specifications of the Integrated Shallot Harvester		
No.	Parameter	Value
1	Width of shallot-contacting component	897.6 cm
2	Distance between shallot-lifting tines	3 mm
3	Width of transport conveyor belt	45 cm
4	Number of transport buckets	16
5	Transport bucket dimensions	(27 × 1.5 × 0.7) cm
6	Soil sieve dimensions	(85 × 95) cm

Modeling of the Integrated Shallot Harvester (ISH)

The ISHM is modeled as a mechanical system consisting of the tractor, harvesting unit, harvesting head, the coupling joint between the tractor and the working machine, and eight wheels. The model has 17 degrees of freedom (DOF) to describe the full motion of the system. Excitation forces from the ground are considered with nonlinear factors, including soil sinkage behavior and wheel–soil interaction modeled using the Bekker theory. A schematic of the dynamic model of the ISH is shown in Fig. 2.

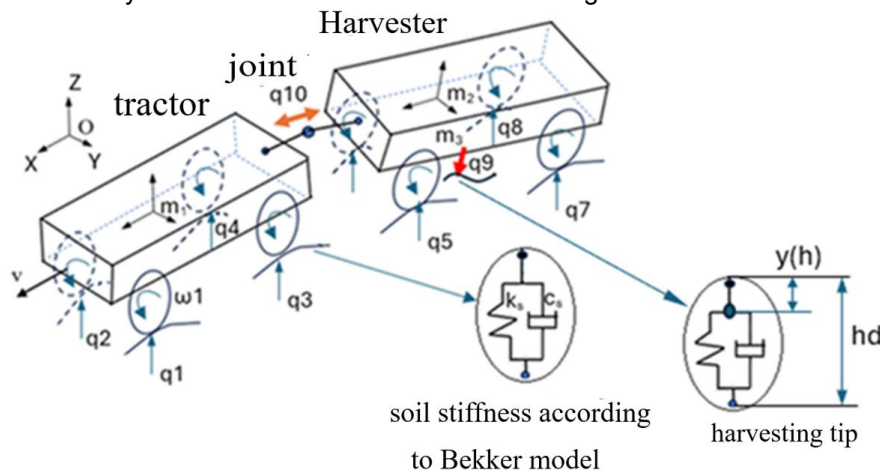


Fig. 2 - Dynamic Model of the Integrated Shallot Harvester

The DOF correspond to the generalized coordinates of the system as follows:

- Tractor: 4 DOF - $x_1, z_1, \varphi_1, \theta_1$ (translation in the x and z -directions, pitch angle, and roll angle)
- Harvester: 4 DOF - $x_2, z_2, \varphi_2, \theta_2$ (translation in the x and z -directions, pitch angle, and roll angle)
- Harvesting head: 1 DOF - z_3 (vertical motion corresponding to digging depth h_d)
- Wheels: 8 DOF (rotational motion around the wheel axis)

The forces acting on the system, based on the Bekker soil interaction model, include:

- Forces from the field surface on the 4 tractor wheels: q_1, q_2, q_3, q_4
- Forces from the field surface on the 4 harvester wheels: q_5, q_6, q_7, q_8
- Force from the field surface on the harvesting head: q_9
- Coupling force at the joint between tractor and harvester: q_{10}

Formulation of the System's Dynamic Equations

Based on the Newton–Euler dynamics principle, the system of differential equations corresponding to the 17 degrees of freedom is presented in Equations (2) to (11).

Equations of Motion for the tractor:

$$m_1 \ddot{z}_1 = q_1 + q_2 + q_3 + q_4 - m_1 g - q_{10-z} \quad (2)$$

$$m_1 \ddot{x}_1 = -q_{9-x} - q_{10-x} \quad (3)$$

$$I_{1-y} \ddot{\varphi}_1 = q_3 \frac{c_1}{2} + q_4 \frac{c_1}{2} - q_1 \frac{c_1}{2} - q_2 \frac{c_1}{2} - q_{10-z}(L_1 - L_{kn}) - q_{10-x} h_1 \quad (4)$$

$$I_{1-x} \ddot{\theta}_1 = q_2 \frac{b_1}{2} + q_4 \frac{b_1}{2} - q_1 \frac{b_1}{2} - q_3 \frac{b_1}{2} \quad (5)$$

where:

z_1 : vertical displacement of the tractor;

I_{1-y} : moment of inertia of the tractor about the y-axis;

I_{1-x} : moment of inertia of the tractor about the x-axis;

L_{kn} : distance from the coupling joint to the front of the tractor.

Equations of motion for the harvester:

$$m_2 \ddot{z}_2 = q_5 + q_6 + q_7 + q_8 - m_2 g + q_{10-z} - q_{9-z} \quad (6)$$

$$m_2 \ddot{x}_2 = q_{9-x} + q_{10-x} \quad (7)$$

$$I_{2-y} \ddot{\varphi}_2 = q_7 \frac{c_2}{2} + q_8 \frac{c_2}{2} - q_5 \frac{c_2}{2} - q_6 \frac{c_2}{2} + q_{10-z}(L_{kn2}) - q_{9-z}(L_2 - st_x) - q_{9-x} h_2 \quad (8)$$

$$I_{2-x} \ddot{\theta}_2 = q_6 \frac{b_2}{2} + q_8 \frac{b_2}{2} - q_5 \frac{b_2}{2} - q_7 \frac{b_2}{2} - q_{9-z} st_y \quad (9)$$

where:

z_2 : vertical displacement of the harvester;

I_{2-y} : moment of inertia of the harvester about the y-axis;

I_{2-x} : moment of inertia of the harvester about the x-axis;

L_{kn2} : distance from the coupling joint to the front of the harvester;

st_x, st_y : coordinates of the harvesting mechanism.

Equation of motion for the harvesting head:

$$m_3 \ddot{z}_3 = q_9 - m_3 g \quad (10)$$

where:

z_3 : vertical displacement of the harvesting mechanism

Equations of motion for the eight wheels:

$$I_{bx} \dot{\omega}_i = r_{bx} q_i \quad (i = 1, 2, \dots, 8) \quad (11)$$

where:

I_{bx} : moment of inertia of the wheels;

$\dot{\omega}_i$: angular acceleration of the i^{th} wheel;

r_{bx} : wheel radius.

Excitation Forces Acting on ISHM Components

Soil Sinkage:

The Bekker mechanical model is used to calculate the soil stiffness (sinkage resistance) under the load of the ISH, as expressed in Equation (12) (Gerhart, 1990).

The authors introduced Bekker's Derived Terramechanics Model (BDTM) to evaluate the mobility performance of ground vehicles, including the ISHM. This approach utilizes seven soil parameters rather than a single index with traditional coefficients, allowing for more detailed comparisons of vehicle mobility performance across various operating conditions.

$$p = k_c \left(\frac{z}{b} \right)^n \quad (12)$$

where:

p : contact pressure (kN/m²);

k_c : soil modulus of deformation (kN/m⁽ⁿ⁾), consisting of two components: k_1 is horizontal modulus, representing the cohesive properties of the soil - its ability to resist sinkage under loading, which reflects soil stiffness; k_2 is vertical modulus, representing the frictional properties of the soil—its resistance to vertical deformation under load;

z : sinkage depth (m);

b : contact width (approximated by the wheel width - m);

n : the soil deformation exponent, which characterizes the nonlinear relationship between stress and strain under loading; it defines the degree of nonlinearity in the soil's response to pressure.

Typical values for loose soil conditions in shallot harvesting fields:

$k_1 = 0.9\text{-}2.5$ kN/m⁽ⁿ⁺¹⁾, assumed value: 1.5;

$k_2 = 1.5\text{-}3.0$ kN/m⁽ⁿ⁺²⁾, assumed value: 2.25;

$n = 0.9\text{-}1.2$, assumed value: 1.

Wheel-Soil Interaction Forces:

Based on the Bekker model, the vertical reaction forces q_i ($i = 1, 2, \dots, 8$) acting on the wheels of the ISHM are calculated using Equation (13).

$$q_i = A \cdot p = A \cdot k_c \left(\frac{z}{b} \right)^n \quad (13)$$

where:

A : effective contact area between the wheel and the ground;

z : sinkage depth of the wheel;

b : wheel width;

k_c, n : soil parameters characterizing stiffness and nonlinearity.

Forces Acting on the Harvesting Head:

Similarly, the forces acting on the harvesting head in the x and z-directions, corresponding to longitudinal and vertical soil stiffness, are calculated using Equation (14).

$$\begin{aligned} q_{9-z} &= k_9(h_d \cdot y(h) - z_3 + z_2 + st_y \cdot \theta_2 - st_x \cdot \varphi_2) \\ q_{9-x} &= c_9 \cdot v \end{aligned} \quad (14)$$

where:

k_9 : soil stiffness at the harvesting head;

c_9 : soil damping coefficient;

h_d : field depth (0.3 m);

$y(h)$: relative depth of the harvesting head;

v : travel speed (5 km/h).

Forces Acting on the Coupling Joint:

Similarly, the forces acting on the coupling joint in the x and z-directions are calculated using Equation (15):

$$\begin{aligned} q_{10-z} &= k_{10}(z_2 - z_1 - L_1\varphi_1 + L_3\varphi_2) \\ q_{10-x} &= k_{10}(x_2 - x_1 - h_1\varphi_1 + h_3\varphi_2) \end{aligned} \quad (15)$$

where:

k_{10} : stiffness of the coupling joint;

L_1, L_3 : distance from the center of mass to the coupling joint;

h_1, h_3 : height of the center of mass.

RESULTS

Nonlinear Analysis and Selection of Solution Method

The ISHM model is a nonlinear dynamic system. The degree of nonlinearity in the model is influenced by multiple factors that affect the vibration behavior of the system (Wong, 2001). This work provides a comprehensive description of vehicle dynamics and road interaction for mechanical systems. It synthesizes and extends models developed by Bekker and other researchers, forming the theoretical foundation for multi-degree-of-freedom dynamic modeling in this study.

Specifically, the nonlinear factors affecting the ISHM model include:

- The soil reaction force is modeled by the Bekker equation, which is nonlinear to z^n .
- Soil resistance at the harvesting head, which exhibits nonlinear behavior.
- Coupling joint force, modeled with elastic stiffness, introduces dynamic response due to relative motion between components.

- Road-induced excitation modeled according to ISO 8608 (random vibration) (ISO 8608, 1995). This international standard classifies and quantifies road surface roughness into eight categories (A–H). It is applied in the study to simulate Category D agricultural terrain with representative surface irregularities.

- Wheels encountering sudden terrain irregularities, introducing impact-like excitation (Pacejka, 2006). The Magic Formula tire model is used to describe tire–terrain interaction, accounting for tires' slip behavior on soft soil.

Model Parameter Identification

The parameters of the model were determined based on the pilot-scale prototype of the ISH, and are as follows:

- Mass of the tractor: $m_1 = 1600$ kg (excluding the four wheels);
- Mass of the harvester unit: $m_2 = 600$ kg (including its four wheels);
- Mass of the harvesting head: $m_3 = 80$ kg (fixed to the harvester frame, operating similarly to a plow blade);
- Mass of each wheel: $m_{bx} = 10$ kg;
- Mass of the coupling joint: $m_k = 30$ kg;
- Tractor dimensions: *Length* \times *Width* \times *Height* ($L_1 \times B_1 \times H_1$) = $2.0\text{ m} \times 1.2\text{ m} \times 1.6\text{ m}$.
- Wheel track (front/rear): $b_1 \times c_1 = 1.2\text{ m} \times 1.4\text{ m}$;
- Wheel radius (front/rear): $r_{bx11}/r_{bx12} = 0.3/0.5\text{ m}$;
- Center of mass height (symmetrical along the longitudinal plane): $h_1 = 0.9\text{ m}$;
- Harvester unit dimensions: *Length* \times *Width* \times *Height* ($L_2 \times B_2 \times H_2$) = $1.6\text{ m} \times 1.0\text{ m} \times 1.4\text{ m}$;
- Wheel track (front/rear): $b_2 \times c_2 = 1.1\text{ m} \times 1.1\text{ m}$;
- Wheel radius (front/rear): $r_{bx21}/r_{bx22} = 0.6/0.15\text{ m}$;
- Center of mass height (symmetrical along the longitudinal plane): $h_2 = 0.6\text{ m}$;
- Harvesting head coordinates: $st_x = b_2/2$; $st_y = c_2/2$;
- Penetration depth of the harvesting head into the soil: $h_t = h_d \cdot y(h)$, where $h_d = 0.3\text{ m}$ is the nominal field depth, and $y(h)$ is a variable penetration factor depending on real-time field interaction during operation.

Model Assumptions

The following assumptions were applied in the model:

- At the initial moment of system operation, the relative penetration factor is set to $y(h)=0.1$ m, so that the initial digging depth h_t is fixed and subsequently varies with $y(h)$.
- The harvesting head is assumed to be perfectly rigid, with no deformation.
- Dimensions of the towing joint: *Length* \times *Height* ($L_3 \times H_3$) = $0.6\text{ m} \times 0.1\text{ m}$;
- Center of mass height of the towing joint (symmetrical along the longitudinal plane): $h_3 = 0.6\text{ m}$;
- The tractor and the harvesting unit are connected by a rotational joint (revolute coupling);
- The system operates over a soil surface path length of $L_d = 30\text{ m}$;
- Soil parameters: Soil stiffness: $k_s = 3000$; Soil damping coefficient: $c_s = 100000$;
- In addition to Bekker sinkage behavior, road excitations include surface irregularities modeled using ISO 8608, Category D, with varying conditions for each wheel throughout the travel path; sinusoidal bumps: Amplitude $h_{x1} = 0.12\text{ m}$ over length $L_{d1} = 8\text{ m}$; Amplitude $h_{x2} = 0.2\text{ m}$ over length $L_{d2} = 15\text{ m}$;
- Maximum longitudinal velocity along the x-direction: $v = 5\text{ km/h}$.

Result Analysis

Dynamic Vibration of the System:

Modern numerical simulation tools were used to solve the system of dynamic differential equations governing the harvester model. The Runge–Kutta method was selected due to its computational efficiency and ease of implementation in MATLAB. The basis for selecting the Runge–Kutta method for solving nonlinear differential equations is supported by *Chauhan & Srivastava (2019)*, who provided theoretical justification for its suitability in complex dynamic system simulations.

The simulation results of the system's dynamic behavior are illustrated in Fig. 3.

The graphs show that large-amplitude oscillations occur during the initial time frame (0-0.5 seconds), then gradually diminish toward zero, indicating that the system stabilizes. This implies that the damping in the system is sufficiently high to suppress oscillations. Frequency analysis reveals 3-4 oscillations within the first second, suggesting a natural frequency of approximately 3-4 Hz. The oscillations are almost entirely damped out within 2.5 seconds, indicating that the damping coefficient $c_s = 300$ Ns/m for the wheels is appropriate for suppressing vibrations.

The tractor unit exhibits minimal vibration, primarily due to elastic excitation from the ground via the soil stiffness, k_s . The large mass of the tractor (1200 kg) leads to high inertia, resulting in low-frequency, small-amplitude, phase-lagged responses relative to the excitation. The harvester unit shows larger vibration amplitudes than the tractor due to its lower mass (500 kg). The coupling joint stiffness contributes to the overall system stiffness, causing resonant-like behavior in the harvester's response (q_2). The harvesting head experiences forced vibrations induced solely by the soil. Due to its small mass, it exhibits relatively strong vibrations. Initially, the head shows large displacement amplitudes (about 0.1 m), which may negatively affect the harvesting process-causing mechanical damage to the machine or bruising the shallots due to excessive impact with the soil.

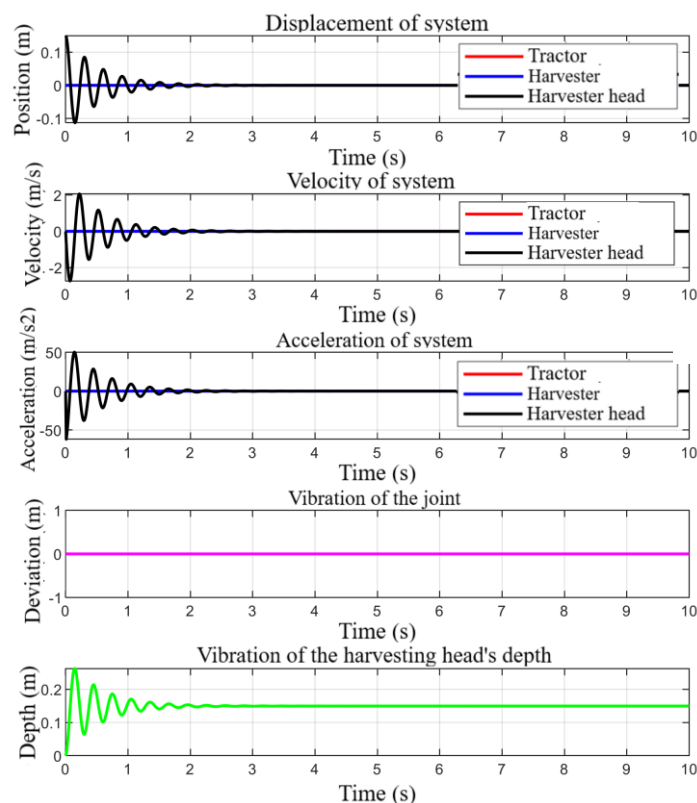


Fig. 3 - Simulated Dynamic Response of the System

The vibration velocity follows a similar trend to the displacement response, with an initially high amplitude of approximately 2 m/s for the harvesting head. Frequency analysis again reveals 3-4 oscillations within the first second, confirming a natural frequency of approximately 3-4 Hz. The velocity decreases rapidly after each oscillation cycle, reaching near-zero levels within approximately 2.5 seconds. The tractor exhibits low vibration velocity, characterized by a slow and smooth response due to its high mass and relatively low velocity frequency. The harvester unit shows relatively larger vibration velocities, reflecting its greater sensitivity to excitation.

Notably, certain segments show clearly defined velocity ripples, which correspond to impulsive excitations caused by surface irregularities. The harvesting head exhibits strong velocity oscillations with large amplitude, especially when directly encountering sinusoidal or pulse-shaped bumps.

The initial vibration acceleration of the harvesting head reaches up to $\pm 50 \text{ m/s}^2$, then gradually diminishes and approaches a quasi-steady state. The peak acceleration amplitude of 50 m/s^2 is considered relatively high compared to typical operational thresholds for mechanical systems used in agriculture. Based on the presence of 3-4 oscillation cycles within the first second, the estimated natural frequency remains around 3-4 Hz. Each oscillation cycle shows a rapid reduction in amplitude-approximately 50% per cycle, indicating effective damping behavior. This raises a critical need to implement design improvements, including: evaluating the fatigue strength of the harvesting structure, introducing an active damping system or impact absorption unit, reducing initial excitation levels or increasing the damping coefficient c_s . These measures are essential to minimize excessive accelerations, enhance system durability, and protect the shallot bulbs from damage during the harvesting process.

The vibration graph of the coupling joint shows that its oscillation amplitude remains close to zero throughout the entire simulation period (0 to 10s), with no significant variation or large fluctuations. This indicates that the connection between the tractor and the harvester operates stably, with no significant phase difference, and no abnormal elongation or compression that could lead to fatigue or mechanical failure of the joint. The rigid coupling ensures structural integrity, and based on this observation, the influence of the coupling joint can be neglected in the analysis. The simulation focus can thus be directed primarily toward the vibrations of the harvester body and the harvesting head.

Harvesting Depth of the Digging Head:

The harvesting depth of the digging head is a critical parameter, reflecting the operational capability of the ISHM. It is directly related to the design of the machine and strongly affects both the quality and efficiency of the harvesting process. Ideally, the digging depth h_d should remain stable, but in practice, it varies along the z -axis due to system vibrations. This variation is referred to as the depth error, denoted by $h(y)$. When the harvesting mechanism undergoes significant vibration, $h(y)$ also fluctuates strongly, resulting in unstable harvesting depth, which can cause premature cutting (if too shallow) or bulb breakage (if too deep). If the vibration-induced variation in depth exceeds $\pm 0.05 \text{ m}$, mechanical interventions are required, such as increasing system stiffness, adding damping mechanisms, and implementing active control strategies. To reduce the initial vibration amplitude and improve harvest quality, the system should be optimized in terms of the damping coefficient (c_s), soil stiffness (k_s), or by deploying real-time active depth control using depth sensors and actuator-based mechanisms for continuous adjustment. An illustration of this behavior is shown in Fig. 4.

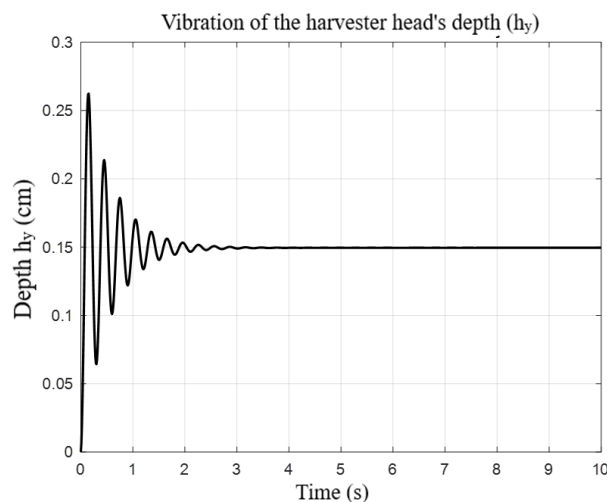


Fig. 4 - Vibration Response of the Harvesting Head

The graph shows that during the initial harvesting phase (0 to 2.5 s), the variation in digging depth is clearly noticeable. The vibration amplitude increases rapidly from 0 to over 0.25cm, before stabilizing as the tractor and harvester reach steady-state operation. If such behavior were to occur in real-world field conditions, it could pose a risk of damaging the shallot bulbs, particularly during the initial moments of harvesting operations when the ISHM first engages with the soil.

Fig. 5 illustrates the relationship between the mass of each component of the ISHM and the vehicle's travel speed, and how these factors affect the digging depth of the harvesting head.

It is evident that the digging depth is significantly influenced by the mass distribution of the system and its operating velocity.

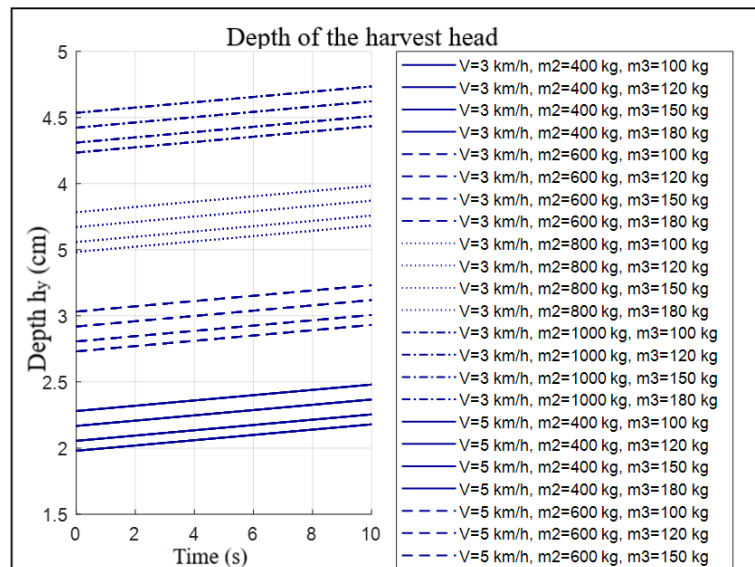


Fig. 5 - Graph of the Influence of Speed and Mass on the Digging Depth of the Harvesting Head

CONCLUSIONS

By developing a 17 DOFs dynamic model for the ISHM, in combination with the Bekker soil sinkage model and surface irregularities including sinusoidal, pulse-shaped, and ISO 8608-based terrain profiles, this study successfully captured the nonlinear interactions between the wheels and the soil, as well as the resistive forces acting on the wheels and the harvesting head.

The main parameters influencing the vibration dynamics and the harvesting quality include the mass of the tractor, harvester, and harvesting head, the travel velocity, the soil stiffness, and the damping coefficient of the system. The overall system exhibits a natural frequency of approximately 3-4 Hz, with vibrations effectively damped within about 2.5s due to the selected damping coefficient of $c_s = 300$ Ns/m, indicating that the current damping design is reasonably effective for suppressing oscillations.

When the ISHM begins operation, the harvesting head exhibits vibration amplitudes up to 0.1 m, with a peak acceleration reaching 50 m/s^2 . The digging depth h_d fluctuates along the z -axis, with an initial variation amplitude of up to 0.25 cm, which exceeds the acceptable depth error threshold of $\pm 0.05 \text{ m}$. This level of vibration may damage shallot bulbs or even cause structural failure of the digging head, especially during the initial phase of harvesting. Therefore, this period represents a critical window in designing and evaluating real-world operating conditions.

The coupling joint between the tractor and the harvester unit operates stably, showing no significant vibration or variation, confirming that the current joint design is structurally sound.

Recommendations for improving harvesting performance: increase the structural stiffness of the harvesting head mechanism; integrate an active damping system to reduce initial vibration effects; design a depth control system that uses sensors and actuators to maintain a stable digging depth h_d dynamically; optimize the operating speed to within the range of 2–4 km/h, which has been shown to reduce vibration and improve harvesting quality.

ACKNOWLEDGEMENT

The authors would like to express their sincere gratitude to Vinh Long University of Technology Education for providing support and favorable conditions for this study.

REFERENCES

- [1] Bekker M. G., (1969). *Introduction to Terrain-Vehicle Systems*. The University of Michigan Press.
- [2] Cardei P., Constantin N., Muraru V., Persu C., Sfiru R., Vladut N., Ungureanu N., Matache M., Muraru-Ionel C., Cristea O., Laza E., (2023). The random vibrations of the active body of the cultivators,

- Agriculture*, vol.13, no.8, article 1565, MDPI / Switzerland. DOI: <https://doi.org/10.3390/agriculture13081565>
- [3] Chauhan V., Srivastava P. K., (2019). Computational techniques based on Runge-Kutta method of various order and type for solving differential equations, *International Journal of Mathematical, Engineering and Management Sciences*, vol. 4, no. 2, pp. 375–386. doi: <https://doi.org/10.33889/IJMEMS.2019.4.2-030>
 - [4] Erokhin M., Dorokhov A., Sibirev A., Aksenov A., Mosyakov M., Sazonov N., Godyaeva M., (2022). Development and Modeling of an Onion Harvester with an Automated Separation System, *AgriEngineering*, vol. 4, no. 2, pp. 380–399, Jun. DOI: <https://doi.org/10.3390/agriengineering4020026>
 - [5] Gerhart G., (1990). Bekker's Terramechanics Model for Off-Road Vehicle Research, *US Army TARDEC*. Available: <https://www.researchgate.net/publication/235069513>
 - [6] ISO 8608:1995, (1995). Mechanical vibration-Road surface profiles - reporting of measured data, *The International Organization for Standardization*.
 - [7] Khura T., Mani I., Srivastava A. P., (2011). Design and development of tractor-drawn onion (*Allium cepa*) harvester, *The Indian Journal of Agricultural Sciences*, vol. 81, no. 6, pp. 44–48, Jun. Available: <https://www.researchgate.net/publication/267251851>
 - [8] Kumawat L., Raheman H., (2023). Determination of engineering properties of onion crop required for designing an onion harvester, *Cogent Engineering*, vol. 10, no. 1. DOI: <https://doi.org/10.1080/23311916.2023.2191404>
 - [9] Marin E., Cârdei P., Vlăduț V., Biriș S., Ungureanu N., Bungescu S., Voicea I., Cujbescu D., Găgeanu I., Popa L., Isticioaia S., Matei G., Boruz S., Teliban G., Radu C., Kabas O., Caba I., Maciej J., (2024). Research on the influence of the main vibration-generating components in grain harvesters on the operator's comfort, *INMATEH Agricultural Engineering*, vol.74, no.3, pp.808–823, Bucharest/Romania. DOI: <https://doi.org/10.35633/inmateh-74-71>
 - [10] Massah J., Arabhosseini A., (2012). Effect of Blade Angle and Speed of Onion Harvester on Mechanical Damage of Onion Bulbs, *Agricultural Mechanization in Asia, Africa & Latin America*, vol. 43, pp. 60–63. Available: <https://www.researchgate.net/publication/287778155>
 - [11] Mehta T. D., Yadav R., (2015). Development and Performance Evaluation of Tractor Operated Onion Harvester, *Agricultural Mechanization in Asia, Africa & Latin America*, vol. 46, no. 4, pp. 7–13, Dec. Available: <https://www.researchgate.net/publication/296259068>
 - [12] Můčka P., (2018). Simulated road profiles according to ISO 8608 in vibration analysis, *Journal of Testing and Evaluation*, vol. 46, no. 1, pp. 405–418. DOI: <https://doi.org/10.1520/JTE20160265>
 - [13] Pacejka Han B., (2006). *Tyre and Vehicle Dynamics*, 2nd ed. Butterworth-Heinemann.
 - [14] Phi C. H., (2021). Research on technology and equipment for high-tech vegetable and fruit production towards automation and compatibility with growing conditions in the Southwest, *Ministry of Science and Technology*.
 - [15] Phi C. H., Hau L. T., Long C. D., (2022). Design and dynamics calculations of shallot seed feeding mechanism, *Engineering Solid Mechanics*, vol. 10, no. 1, pp. 71–78. DOI: <https://doi.org/10.5267/j.esm.2021.10.001>
 - [16] Phi C. H., Van N. T., Ky L. H., (2020). Design and Manufacturing of a Non-Standard Chain Parts for a Chain Conveyor for a Harvest Shallot: A Case Study, *Applied Mechanics and Materials*, vol. 902, pp. 91–96. DOI: <https://doi.org/10.4028/www.scientific.net/AMM.902.91>
 - [17] Rashidi M. et al., (2012). Evaluation of Bekker model in predicting soil pressure-sinkage behaviour under field conditions, *Middle East Journal of Scientific Research*, vol. 12, no. 10, pp. 1364–1369. DOI: <https://www.idosi.org/mejsr/mejsr12%2810%2912/9.pdf>
 - [18] Vlăduț N.-V. et al., (2023). Considerations regarding the effects of shocks and vibrations on operators of self-propelled agricultural equipment, *INMATEH Agricultural Engineering*, vol.71, no.3, pp.843–856, Bucharest/Romania. DOI: <https://doi.org/10.35633/inmateh-71-74>
 - [19] Vlăduț V., Biriș S.-Ș., Bungescu S.T., Herișanu N., (2013). Influence of vibrations on the operator in the grain harvesters, *Applied Mechanics and Materials*, vol.430, pp.290–296, Switzerland. DOI: <https://doi.org/10.4028/www.scientific.net/AMM.430.290>
 - [20] Wong J. Y., (2001). *Theory of ground vehicles*, 3rd ed. John Wiley.